Conversion dependent morphology predictions for composite emulsion polymers: 2. Artificial latices

Catherine L. Winzor and Donald C. Sundberg*
Polymer Research Group, Department of Chemical Engineering, University of New Hampshire, Durham, NH 03824, USA
(Received 1 February 1991; accepted 5 November 1991)

An equilibrium thermodynamic analysis of composite particle morphology development within artificial latices is presented. The analysis emphasizes the role of the solvent upon phase compositions and interfacial tensions, and predictions of the favoured morphology are made as a function of the extent of solvent removal. Experimental observations of the morphology of poly(methyl methacrylate)/polystyrene composite particles agree well with the predictions and demonstrate the significant role that the surfactant can have upon the preferred particle structure. Consideration is given to the choice of solvent used to produce the artificial latex and it is predicted that the preferred particle morphology is unlikely to be dependent upon the type of solvent used in the process.

(Keywords: latex; particle morphology; solvent; interfacial tensions)

INTRODUCTION

The control of structured latex particle morphology is critical in achieving desirable physical properties for coatings, impact resistant plastics and other applications. Given that a number of morphologies are possible[1–9] and that a variety of processes are used to produce the latices, there is a clear need to develop an ability to predict composite particle morphology. Two very different methods of producing composite latex particles are the synthetic and artificial routes. In the former, monomer is added to a seed latex and polymerization is carried out to form the second polymer in the presence of the first polymer. Phase separation occurs during the polymerization reaction and particle morphology develops accordingly. In the latter route, two preformed polymers are dissolved in a mutual solvent, emulsified into water containing a surfactant, and the solvent subsequently removed by evaporation. In this instance phase separation occurs as the solvent is removed and the particle volume decreases, but the ratio of the two polymers within the particle always remains constant.

We have recently presented a detailed methodology for predicting the morphological structure of composite latex particles derived from the synthetic processing route[10]. The goal of the present discussion is to outline a similar analysis for artificial latex processing. Further, we address the question of whether or not the choice of the type of solvent has an influence upon the particle morphology as it develops during processing. Lastly, we offer some experimental results for which the conversion dependent morphologies are compared to equilibrium thermodynamic predictions, as detailed in this paper.

*To whom correspondence should be addressed

0032-3861/92/204269-11

THERMODYNAMIC CONSIDERATIONS

Recently[11] we presented the derivations of reduced surface energies for several basic morphologies. In a later paper[10] a revised reference state allowed the calculation of reduced surface energies and prediction of equilibrium morphologies (including occluded structures) during polymerization reactions. In this paper, we present the reduced surface energy equations derived for basic and occluded morphologies for polymer composite particles formed via artificial processing routes involving solvent removal.

The basic morphologies are shown in *Figure 1* together with the revised reference state of polymer 1 particles and separate, bulk phases of polymer 2 and solvent. For all of the morphologies represented in *Figure 1*, the change in free energy can be expressed as:

$$\Delta G = \sum_i \gamma_i A_i - \gamma_{P1/W} A'_0 \qquad (1)$$

where γ_i is the interfacial tension of the ith interface and A_i is the corresponding interfacial area. Thus $\gamma_{P1/W}$ is the interfacial tension of the original polymer 1 particle suspended in water (and surfactant) and A'_0 is its interfacial area. The $\gamma_{P1/W}A'_0$ term corresponds to the reference energy state. Each different particle morphology differs only in geometry, leading to different expressions for $\sum_i \gamma_i A_i$. In our earlier paper[11] we obtained expressions for $(\Delta\gamma)$, the reduced free energy change, which was obtained by dividing the expression for ΔG by the reference area:

$$(\Delta\gamma) = \Delta G / A'_0 \qquad (2)$$

The equations were derived in terms of the volume fraction of polymer 2 in the particle (ϕ_p). More recently,

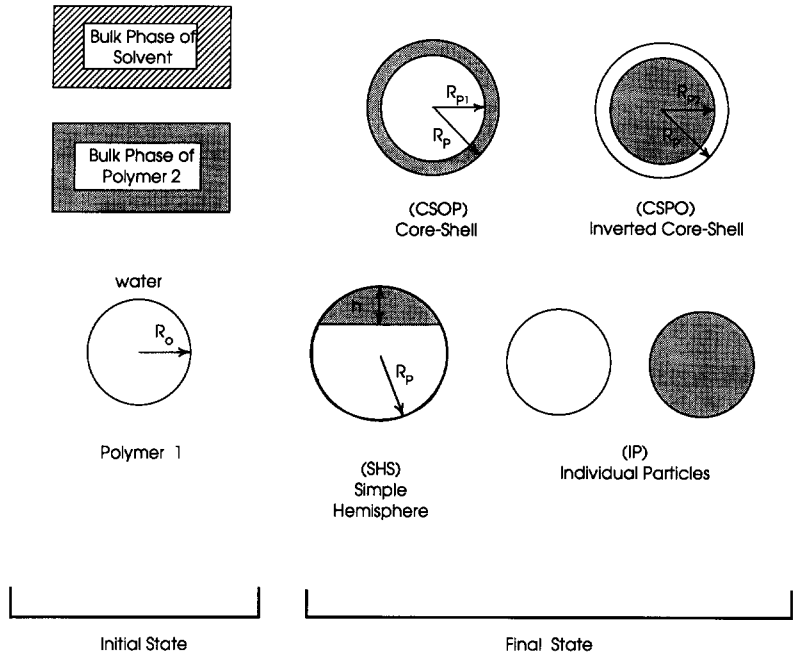

Figure 1 Initial (reference) and final states for morphology development (basic morphologies)

we presented the equations (with a revised reference state) for a polymerizing system (synthetic route), where the reduced free energies were calculated as a function of conversion[10]. Analogously, the reduced free energy equations for the artificial processing route can be derived in terms of the fraction of solvent removed, and are similar to those derived for the synthetic route presented in the previous paper[10].

The reduced free energies for the four basic morphologies of *Figure 1* [core–shell (CSOP), inverted core–shell (CSPO), individual particles (IP) and simple hemisphere (SHS)] are:

$$(\Delta\gamma)_{CSOP} = \gamma_{P1S/P2S}(R_{P1}/R_0)^2 + \gamma_{P2S/W}(R_P/R_0)^2 - \gamma_{P1/W} \quad (3)$$

$$(\Delta\gamma)_{CSPO} = \gamma_{P1S/P2S}(R_{P2}/R_0)^2 + \gamma_{P1S/W}(R_P/R_0)^2 - \gamma_{P1/W} \quad (4)$$

$$(\Delta\gamma)_{IP} = \gamma_{P1S/W}(R_{P1}/R_0)^2 + \gamma_{P2S/W}(R_{P2}/R_0)^2 - \gamma_{P1/W} \quad (5)$$

$$(\Delta\gamma)_{SHS} = 0.5(R_P/R_0)^2\{\gamma_{P1S/P2S}(h/R_P)[1 - 0.5(h/R_P)] + \gamma_{P2S/W}(h/R_P) + \gamma_{P1S/W}[2 - (h/R_P)]\} - \gamma_{P1/W} \quad (6)$$

In order to solve equation (6), the volume ratio of the polymer 2 phase to the total particle [equation (7)] is also required:

$$V_{P2}/V_P = 0.75(h/R_P)^2 - 0.25(h/R_P)^3 \quad (7)$$

Equations (3)–(6) contain terms for the solvent-influenced interfacial tensions ($\gamma_{P1S/P2S}$, $\gamma_{P1S/W}$ and $\gamma_{P2S/W}$) and the interfacial areas (which are dominated by swelling due to the presence of solvent). The effect of solvent on the interfacial tensions will be discussed in a later section. The interfacial area terms are calculated as follows:

$$(R_P/R_0)^2 = (\{(w_{P1}/\rho_{P1}) + [(1 - X)w_S/\rho_S] + (w_{P2}/\rho_{P2})\}/(w_{P1}/\rho_{P1}))^{2/3} \quad (8)$$

$$(R_{P1}/R_0)^2 = \{[(w_{P1}/\rho_{P1}) + (w_{SP1}/\rho_S)]/(w_{P1}/\rho_{P1})\}^{2/3} \quad (9)$$

$$(R_{P2}/R_0)^2 = \{[(w_{P2}/\rho_{P2}) + (w_{SP2}/\rho_S)]/(w_{P1}/\rho_{P1})\}^{2/3} \quad (10)$$

$$V_{P2}/V_P = [(w_{P2}/\rho_{P2}) + (w_{SP2}/\rho_S)]/\{(w_{P1}/\rho_{P1}) + (w_{P2}/\rho_{P2}) + [(1 - X)w_S/\rho_S]\} \quad (11)$$

where X is the fraction of solvent removed, and the w and ρ terms are the masses and densities of each component. The solvent will partition between the polymer phases – hence the terms w_{SP1} and w_{SP2}, which are the masses of solvent in the polymer 1 and polymer 2 phases, respectively.

As was the case for the reactive processing pathway (polymerization), the possibility exists for the formation of incompletely phase-separated structures, i.e. occluded morphologies. Some of these morphologies are shown in *Figure 2*. The corresponding equations for the reduced free energies are:

$$(\Delta\gamma)_{CSPOOCC} = \gamma_{P1S/P2S}N^{1/3}(R_{P1}/R_0)^2 + \gamma_{P2S/W}(R_P/R_0)^2 - \gamma_{P1/W} \quad (12)$$

$$(\Delta\gamma)_{CSPOOCC} = \gamma_{P1S/P2S}N^{1/3}(R_{P2}/R_0)^2 + \gamma_{P2S/W}(R_P/R_0)^2 - \gamma_{P1/W} \quad (13)$$

where N is the number of occlusions. For the sandwich morphology (SHS with two equal lobes):

$$(\Delta\gamma)_{SAND} = (R_P/R_0)^2[\gamma_{P1S/P2S}(h_S/R_P)(1 - h_S/2R_P) + \gamma_{P2S/W}(h_S/R_P) + \gamma_{P1S/W}(1 - h_S/R_P)] - \gamma_{P1/W} \quad (14)$$

where h_S is the height of the sandwich lobe and:

$$V_{P2}/V_P = 1.5(h_S/R_P)^2 - 0.5(h_S/R_P)^3 \quad (15)$$

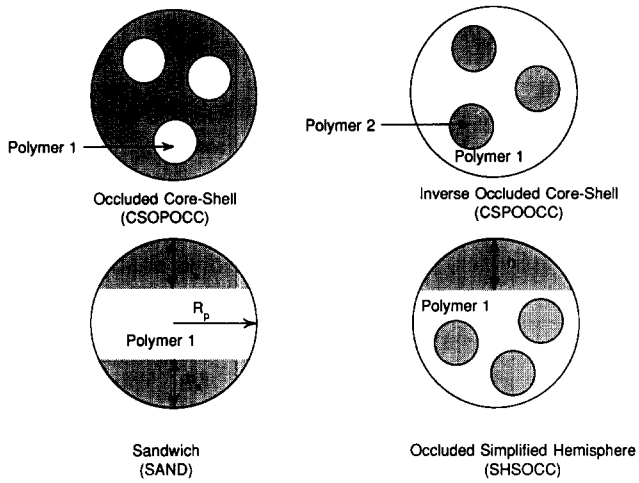

Figure 2 Final states for occluded morphology development

while for the occluded hemisphere morphology:

$$(\Delta\gamma)_{SHSOCC} = 0.5(R_P/R_0)^2[\gamma_{P1S/P2S}((h/R_P)(1 - h/2R_P) + 2N^{1/3}\{[(1 - L)/L][0.75(h/R_P)^2 - 0.25(h/R_P)^3]\}^{2/3}) + \gamma_{P2S/W}(h/R_P) + \gamma_{P1S/W}(2 - h/R_P)] - \gamma_{P1/W} \quad (16)$$

where

$$V_{P2}/V_P = (1/L)[0.75(h/R_P)^2 - 0.25(h/R_P)^3] \quad (17)$$

Here L is the (arbitrary) fraction of polymer 2 in the hemisphere lobe, compared to that in the occlusions.

It can be seen that these reduced surface energy equations require some additional information compared to the original equations of our earlier paper[11]. First, some knowledge of the phase equilibria, i.e. the partitioning of solvent between the polymer phases (and also between the polymer phases and the aqueous phase if the solvent is significantly water soluble) is necessary. Second, the effect of the solvent on the polymer/water (surfactant) and polymer/polymer interfacial tensions must be considered. The amount of solvent present in the composite polymer particles during a typical solvent removal experiment (artificial pathway) is usually quite large and thus the magnitude of these effects is significant and should not be ignored.

INTERFACIAL PROPERTY CONSIDERATIONS

In our previous paper[10], we discussed the effects of monomer on the various interfacial tensions for polymerizing composite particles. In considering the artificial processing pathway of solvent removal from composite particles, solvent is substituted for monomer. Many of the equations that we presented in that paper are equally applicable here (since the monomer was a solvent for the polymerizing system), however, two points lead us to reconsider the effects on the different interfacial tensions. First, there is much more solvent present in the composite particles, thus the effects on interfacial tensions are considerably magnified; second, the amount of polymer 2 in the particles is no longer dependent on the conversion of monomer, remaining constant during processing. Here we will present a condensed version of the equations used to calculate the solvent-influenced interfacial tensions; additional details are given in the paper cited above[10].

Phase compositions

In cases where the solvent is somewhat water-soluble, partitioning of the solvent occurs between the polymer particles and the aqueous phase in which they are suspended, thus reducing the amount of solvent available to partition between the two polymer phases within the composite particles. This phenomenon, if present, must be considered first. Here, for simplicity, we will treat the composite particle as a single, combined phase in order to obtain a first approximation of the solvent distribution. An estimate of the aqueous partition coefficient (P) of the solvent can be obtained from its molal solubility (S), using Hansch parameters[12] and equation (18):

$$\log 1/S = a \log P + b \quad (18)$$

It is then a simple matter to calculate the amounts of solvent in the polymer and aqueous phase (with the constraint that the concentration of solvent in the aqueous phase cannot exceed its solubility).

Having established the amount of solvent in the total polymer phase, the amount in each of the composite phases can be calculated from the tie-lines of the phase diagram. Here we have adopted the approach of Kruse[13], who showed that:

$$(1 - v_3)/(1 - v_2) = e^{(\chi_{12} - \chi_{13})} \quad (19)$$

where v_3 and v_2 are the volume fractions of polymer 1 in the polymer 1 phase ahd polymer 2 in the polymer 2 phase, respectively, and χ_{13} and χ_{12} are the respective solvent/polymer interaction parameters. Estimates of χ_{12} and χ_{13} can be made using solubility parameters[14]. *Figure 3* shows tie-lines calculated for the situation $\chi_{12} = \chi_{13} = 0.40$ using equation (19).

Effect of solvent on interfacial tensions

Once the volume fractions of solvent in each phase have been calculated, the effect on the interfacial tensions can be assessed. Previously[10], we presented a series of equations used to calculate these effects in a reactive system. Since the monomer was, in fact, a solvent for that composite particle system, the equations, and our reasons for selecting them, remain the same.

Polymer/polymer interfaces. In order to calculate the solvent-influenced polymer/polymer interfacial tensions,

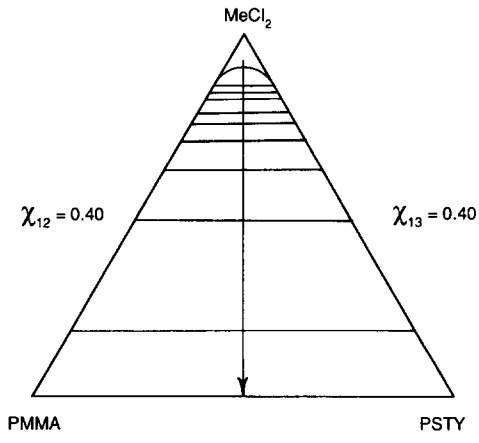

Figure 3 Phase diagram showing tie-lines for 50:50 PMMA/PSTY/$MeCl_2$ particles (10 wt% polymer) at 40°C during artificial processing (solvent removal)

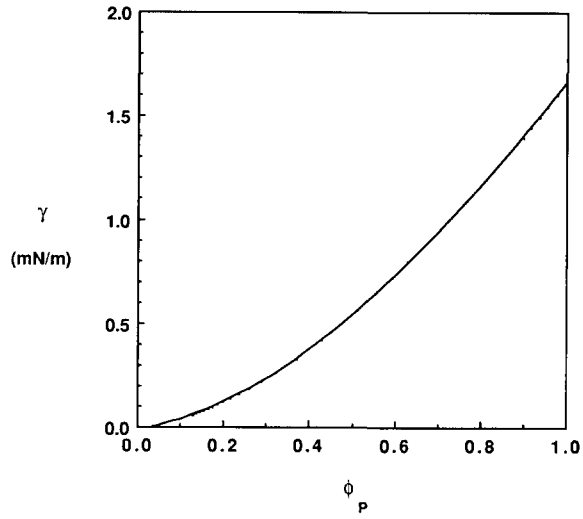

Figure 4 Effect of solvent on the polymer/polymer interfacial tension calculated for 50:50 PMMA/PSTY particles swollen with $MeCl_2$ (10 wt% polymer) along the solvent removal pathway indicated in *Figure 3*

we have adopted equations derived by Broseta *et al.*[15] who adapted mean field equations derived by Helfand *et al.*[16–19] for polymer/polymer interfaces.

$$\gamma_\infty = (kT/\xi^2)(u/6)^{0.5} \quad (20)$$

where u is a concentration dependent Flory polymer/polymer interaction parameter, χ_{23}, and ξ is a correlation length (also concentration dependent). Full details of the calculation sequence for the concentration dependence of these parameters have been presented earlier[10]; a brief description is given in the Appendix of this paper.

A calculated profile for the solvent-influenced polymer/polymer interfacial tension during solvent removal is shown in *Figure 4* for 50:50 poly(methyl methacrylate)/polystyrene (PMMA/PSTY) particles swollen with methylene chloride ($MeCl_2$) (10 wt% total polymer initially). In these calculations it was assumed that both polymers were of equal molecular weight ($\bar{M}_n = 100000$) and a polymer/polymer interaction parameter for the solvent-free polymer particles (pure blend) $\chi_{23} = 0.04$ (consistent with the measurements of Russell *et al.*[20]) was used. The calculated interfacial tension rises by two orders of magnitude during the solvent removal, from 10^{-2} mN m^{-1} at high concentrations of solvent to 1.7 mN m^{-1} for the solvent-free particles.

Polymer/water interfaces. Previously[10] we adopted equations derived by Siow and Paterson[21] (based on a lattice theory approach developed by Prigogine and Marechal[22] and refined by Gaines[23,24]) to predict the effect of monomer on the polymer/water interfacial tensions. The equations of interest are:

$$\ln[(\phi_2^s/\phi_2)^{1/r}/(\phi_1^s/\phi_1)] = [(\gamma_1 - \gamma_2)a]/kT + \chi(l+m)(\phi_1^2 - \phi_2^2) - \chi l[(\phi_1^s)^2 - (\phi_2^s)^2] \quad (21)$$

$$[(\gamma - \gamma_1)a/kT] = \ln[(\phi_1^s)/\phi_1] + [(r-1)/r](\phi_2^s - \phi_2) + \chi[l(\phi_2^s)^2 - (l+m)\phi_2^2] \quad (22)$$

where ϕ_i is the bulk phase volume fraction of component i, ϕ_i^s is the volume fraction of component i in the surface (interface) phase, l and m are constants (from lattice theory), a is a molar volume term for the solvent, r is the ratio of the molar volumes of the polymer and solvent and χ is the polymer/solvent interaction parameter. Equation (21) must be solved numerically to obtain ϕ_1^s, the volume fraction of solvent adsorbed at the interface; the interfacial tension is then calculated via equation (22). If $\gamma_2 > \gamma_1$, then preferential adsorption of solvent will occur at the interface ($\phi_1^s > \phi_1$). In contrast, if $\gamma_2 < \gamma_1$, then the polymer will be preferentially adsorbed. We can now estimate interfacial tensions for solutions of polymers against water containing surfactant. *Figure 5* shows the predicted interfacial tensions calculated for (PMMA, $MeCl_2$)/(water, SLS) and (PSTY, $MeCl_2$)/(water, SLS), where SLS is the surfactant sodium lauryl sulphate. In our calculations we have assumed $\chi_{PMMA/MeCl_2} = \chi_{PSTY/Me2l_2} = 0.40$. The relevant interfacial tensions are: PMMA/(water, SLS) = 13.1 mN m^{-1}, PSTY/(water, SLS) = 13.7 mN m^{-1} and $MeCl_2$/(water, SLS) = 2.0 mN m^{-1}; the polymer/water interfacial tensions were determined by contact angle measurements in this laboratory[11], and that for $MeCl_2$ was more recently measured using a Du Nuoy ring tensiometer. In both cases, $\gamma_2 > \gamma_1$, and preferential adsorption of solvent at the interface is predicted. Changing the surfactant from SLS to the natural pectin, Mexpectin XSS100 (MXP), the measured polymer/water interfacial tensions are: PMMA/(water, MXP) = 15.9 mN m^{-1} and PSTY/(water, MXP) = 37.8 mN m^{-1}, while the measured interfacial tension for $MeCl_2$/(water, MXP) = 6.0 mN m^{-1}. The predicted solvent-influenced interfacial tension curves for this surfactant are shown in *Figure 6*. Again, preferential adsorption of solvent at the interface is predicted for both polymers.

Having assembled thermodynamically sound relationships for the prediction of the influence of solvent on the various interfacial tensions present in solvent-swollen composite polymer particles, we are now in a position to make realistic predictions of equilibrium morphology.

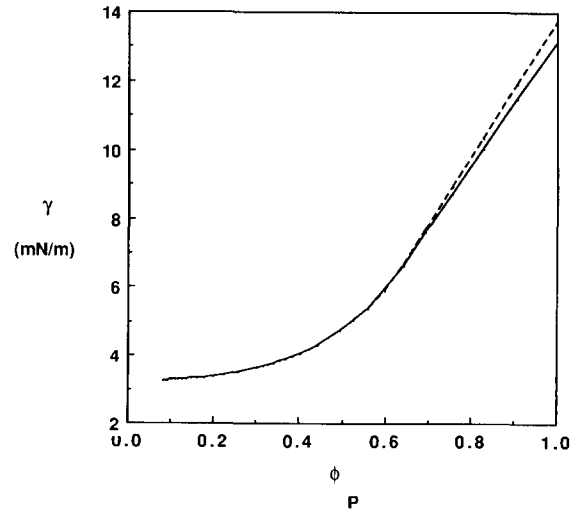

Figure 5 Effect of solvent on the polymer/water interfacial tension (showing preferential solvent adsorption at interfaces); calculated for 50:50 PMMA/PSTY particles swollen with $MeCl_2$ (10 wt% polymer) and suspended in water containing 0.5 wt% SLS as surfactant. (– – –) PSTY,$MeCl_2$/water,SLS; (——) PMMA,$MeCl_2$/water, SLS

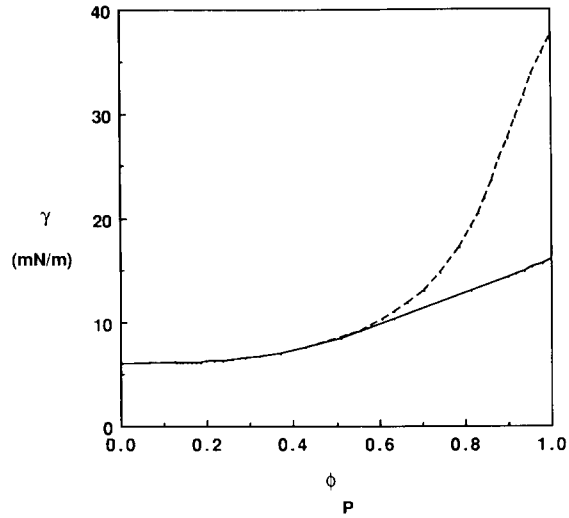

Figure 6 Effect of solvent on the polymer/water interfacial tension showing preferential solvent adsorption at the interfaces; calculated for 50:50 PMMA/PSTY particles swollen with $MeCl_2$ (10 wt% polymer) and suspended in water containing 0.5 wt% MXP XSS100 as surfactant. (——) PMMA, $MeCl_2$/water, MXP; (– – –) PSTY, $MeCl_2$/water, MXP

PREDICTED MORPHOLOGIES DURING SOLVENT REMOVAL

Once the necessary solvent dependences of interfacial tensions and interfacial areas have been derived (as described in the preceding sections), comparison of the $(\Delta\gamma)$ computations provides some useful insights regarding the prediction of composite particle morphologies during solvent removal. We have selected as an example system, composite particles comprising 50:50 (wt/wt) PSTY/PMMA swollen with $MeCl_2$ (initially at 10 wt% polymer), and suspended in water containing one of two surfactants (either SLS or a natural pectin, MXP XSS100). The calculated solvent-influenced interfacial tensions are shown in *Figures 5* and *6*. The corresponding $(\Delta\gamma)$ curves for the three basic morphologies (CSOP, CSPO and SHS) are shown in *Figures 7* and *8*. For both surfactants [SLS (*Figure 7a*) and MXP (*Figure 8*)] the $(\Delta\gamma)$ curves lie very close together until a considerable portion (80%) of solvent has been removed from the particles. In both figures, the hemisphere morphology displays the lowest reduced surface energy [$(\Delta\gamma)$] during the first 80% of solvent removal and would be predicted as the dominant morphology. For the SLS-stabilized particles, the $(\Delta\gamma)_{SHS}$ curve remains that of lowest reduced surface energy through to complete solvent removal. However, for the MXP system at higher fractions of solvent removal (>85%), the CSOP morphology is computed to have the lowest surface energy. In considering these systems, it should be noted that the amount of solvent swelling the particles is large, and that the volume fraction of polymer in the particles does not increase significantly until some 80% of the solvent has been removed. This is reflected in the calculated interfacial tensions of *Figures 5* and *6*, where the curves are solvent-dominated for $\phi_P < 0.4$, corresponding to solvent removal of <80%. Up to this point, all of the $(\Delta\gamma)$ curves for the SLS (*Figure 7a*) and MXP (*Figure 8*) systems are very close together, and the calculated reduced surface energies decrease rapidly. This decrease is due to the significant decrease in particle

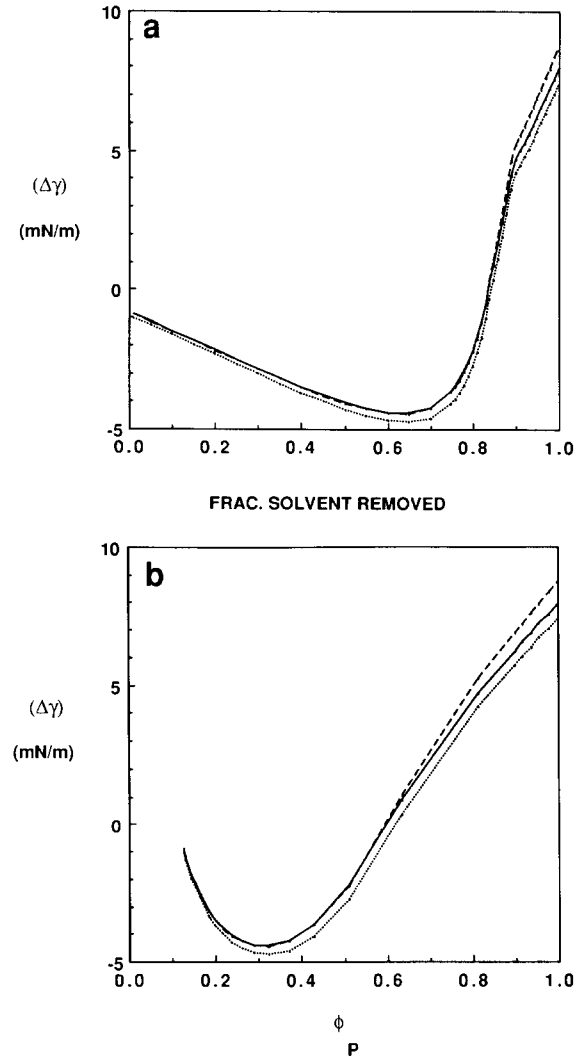

Figure 7 Calculated reduced surface energies [for 50:50 PMMA/PSTY particles swollen with $MeCl_2$ (10 wt% polymer) and suspended in water containing 0.5 wt% SLS as surfactant] for solvent removal at 40°C: (a) plotted against fraction of solvent removed; (b) plotted against total volume fraction of polymer. (——) CSOP; (– – –) CSPO; (· · ·) SHS

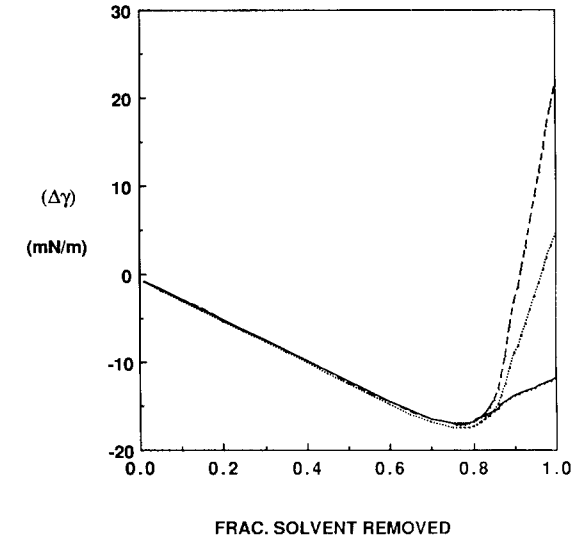

Figure 8 Calculated reduced surface energies [for 50:50 PMMA/PSTY particles swollen with $MeCl_2$ (10 wt% polymer) and suspended in water containing 0.5 wt% MXP as surfactant] for solvent removal at 40°C plotted against fraction of solvent removed. (——) CSOP; (– – –) CSPO; (· · ·) SHS

volume (and interfacial areas) as solvent is removed; the interfacial tensions are solvent-dominated and are practically constant in this region. However, as the volume fraction of polymer increases, the contribution of the changing interfacial tensions to the ($\Delta\gamma$) curves increases. At larger fractions of solvent removal, the ($\Delta\gamma$) curves for the MXP-stabilized particles (*Figure 8*) are easily distinguished, in contrast to the curves of *Figure 7a* for SLS-stabilized particles. A visual improvement for *Figure 7a* is gained by plotting the ($\Delta\gamma$) curves as a function of polymer volume fraction, as shown in *Figure 7b*. This transformation emphasizes the closeness of the solvent-dominated ($\Delta\gamma$) curves at low polymer volume fractions, and gives better visual separation of the curves at high volume fractions.

At low fractions of polymer, the closeness of the different surface energy curves leads to the possibility that several different morphologies may be observed simultaneously, or that any one of the single morphologies may dominate. This is related to the small difference in reduced energies ($\sim 0.5\ mN\ m^{-1}$), which is similar in magnitude to the uncertainties in our measured interfacial tensions. Although this difference between the curves is similar for both surfactant systems, the scale differences between the two sets of curves suggest that the difference may be more significant in differentiating between the ($\Delta\gamma$) curves for the SLS-stabilized particles compared to those for the MXP-stabilized particles.

The probability of finding multiple morphologies existing at one time is further increased when the ($\Delta\gamma$) curves are calculated for the various occluded morphologies of *Figure 2*. *Figures 9* and *10* show that these curves lie between those calculated for the fully phase-separated basic morphologies, as might be expected. For simplicity, not all of the surface energy curves for possible morphologies have been plotted – only those of lowest energy. The small differences in reduced surface energies are due to the influence of solvent on the polymer/polymer interfacial tension and the fact that this interfacial tension is small compared to those for the polymers against water, favouring the formation of occlusions. However, at low polymer fractions, the presence of large amounts of solvent should result in low viscosity and low diffusional resistance, thus seemingly favouring the more fully phase-separated morphologies. At large polymer fractions, the diffusional resistance may increase, as may the possibility of formation of occluded morphologies.

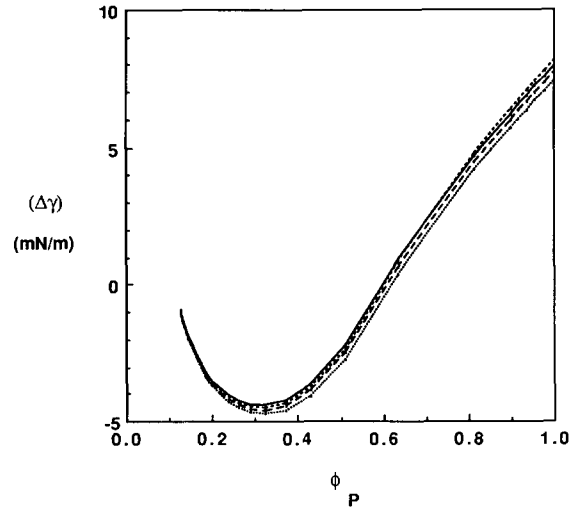

Figure 9 Calculated reduced surface energies for some occluded morphologies [for 50:50 PMMA/PSTY particles swollen with $MeCl_2$ (10 wt% polymer) and suspended in water containing 0.5 wt% SLS as surfactant] for solvent removal at 40°C plotted against total volume fraction of polymer. (——) CSOP; (· · ·) SHS; (– – –) SAND; (–·–) SHSOCC (five occlusions, lobe: 75%)

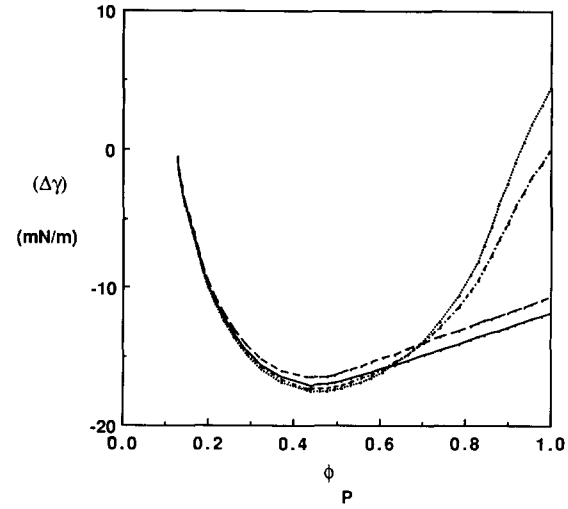

Figure 10 Calculated reduced surface energies for some occluded morphologies [for 50:50 PMMA/PSTY particles swollen with $MeCl_2$ (10 wt% polymer) and suspended in water containing 0.5 wt% MXP as surfactant] for solvent removal at 40°C plotted against total volume fraction of polymer. (——) CSOP; (· · ·) SHS; (–·–) SAND; (– – –) CSOPOCC (five occlusions)

Having noted the strong influence of solvent on the interfacial tensions in the case of $MeCl_2$, where the solvent/water interfacial tensions are very low, it is interesting to consider the same 50:50 PMMA/PSTY particles swollen with toluene (initially at 10 wt% polymer) suspended in water with the same surfactants. The interfacial tensions for toluene/(water, SLS) ($3.2\ mN\ m^{-1}$) and toluene/(water, MXP) ($28.1\ mN\ m^{-1}$) were measured in this laboratory using the drop-weight-volume method. The interfacial tension profiles are shown in *Figures 11* and *12* for SLS- and MXP-stabilized particles, respectively. In *Figure 11* (SLS), there is preferential adsorption of solvent at both polymer/water interfaces (as also occurred with $MeCl_2$). However, on changing surfactant, *Figure 12* shows preferential adsorption of PMMA at the PMMA/water interface, but preferential adsorption of toluene at the PSTY/water interface, in contrast to $MeCl_2$ (*Figure 6*) where the solvent was preferentially adsorbed at both interfaces. The calculated ($\Delta\gamma$) curves for the composite particles swollen with toluene are shown in *Figures 13* and *14* for SLS- and MXP-stabilized particles, respectively. *Figure 13* predicts that toluene-swollen, SLS-stabilized particles will have hemisphere morphology through the entire solvent removal process, as was the case for $MeCl_2$-swollen particles (*Figures 7a* and *b*). When the surfactant is changed to MXP, the ($\Delta\gamma$) curves of *Figure 14* indicate that CSOP morphology has the lowest reduced surface energy for toluene-swollen particles during the entire solvent removal process. This is in contrast to particles swollen by $MeCl_2$, where the possibility of hemisphere morphology for lower volume fractions of polymer was predicted (*Figure 8*).

The reduced surface energy curves of *Figure 14* are

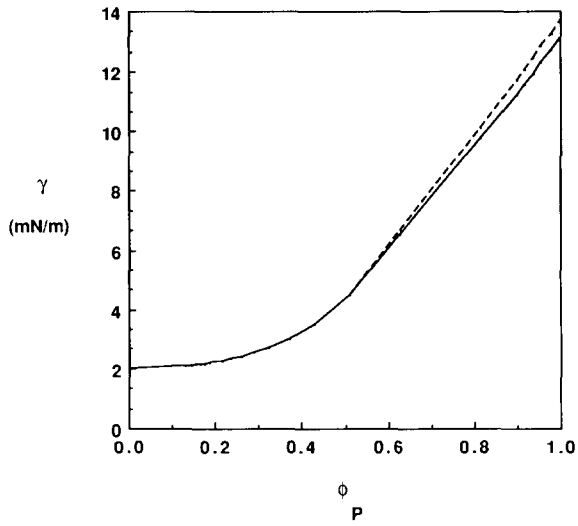

Figure 11 Effect of solvent on the polymer/water interfacial tension (showing preferential solvent adsorption at interfaces); calculated for 50:50 PMMA/PSTY particles swollen with toluene (10 wt% polymer) and suspended in water containing 0.5 wt% SLS as surfactant. (– – –) PSTY, toluene/water, SLS; (——) PMMA, toluene/water, SLS

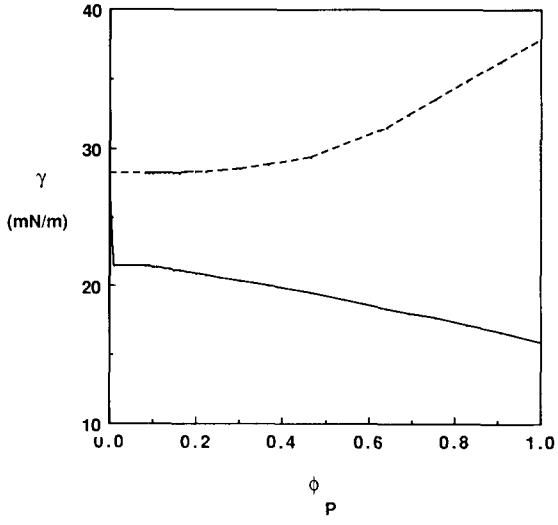

Figure 12 Effect of solvent on the polymer/water interfacial tension displaying both preferential polymer adsorption (——, PMMA/H_2O) and preferential solvent adsorption (– – –, PSTY/H_2O) at the interfaces; calculated for 50:50 PMMA/PSTY particles swollen with toluene (10 wt% polymer) and suspended in water containing 0.5 wt% MXP XSS100 as surfactant

very different in appearance to those in the preceding plots of reduced surface energy (cf. *Figures 7, 8* and *13*). The explanation for this behaviour is found in *Figure 12* and the influence of the solvent on the polymer/(water, surfactant) interfacial tensions. In the $MeCl_2$-swollen particles that we have considered, $MeCl_2$ is preferentially adsorbed at both of the polymer/water interfaces, regardless of surfactant choice (*Figures 5* and *6*). This is also the case for SLS-stabilized PMMA/PSTY particles swollen with toluene (*Figure 11*). However, in the case of toluene-swollen, MXP-stabilized PMMA/PSTY particles, toluene is preferentially adsorbed at the (PSTY, toluene)/(water, MXP) interface while PMMA dominates the (PMMA, toluene)/(water, MXP) interface (*Figure 12*). Fortuitously, these opposing trends (as solvent is removed) in interfacial tension appear to cancel one another, and the reduced surface energy curves of *Figure 14* are dominated by the decrease in interfacial area terms as toluene is removed from the particles.

Thus far, we have considered the possible effects of solvent on morphology development in phase-separating polymer particles. Using artificial processing techniques it is possible to observe the particle morphology as the solvent is quantitatively removed. In the following section we document the results of such experiments for $MeCl_2$-swollen PMMA/PSTY particles as $MeCl_2$ is removed, and compare our free-energy based predictions with these results.

EXPERIMENTAL

Procedure

PMMA (Eastman Kodak, $\bar{M}_n = 102\,000$, $\bar{M}_w/\bar{M}_n = 5.9$) and PSTY (Aldrich, $\bar{M}_n = 82\,700$, $\bar{M}_w/\bar{M}_n = 3.2$) were dissolved in $MeCl_2$ (Baker, h.p.l.c. grade) to give

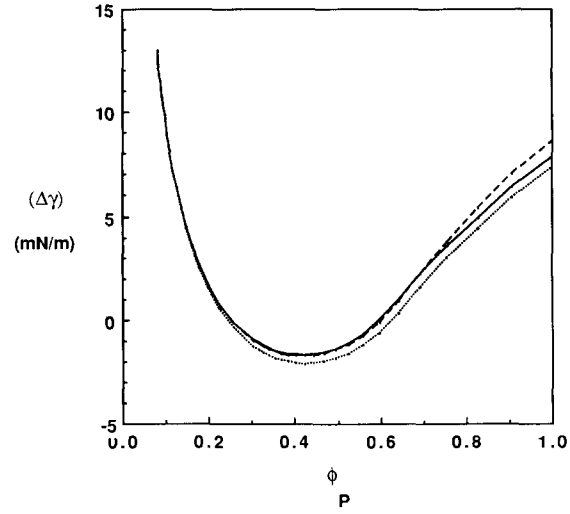

Figure 13 Calculated reduced surface energies [for 50:50 PMMA/PSTY particles swollen with toluene (10 wt% polymer) and suspended in water containing 0.5 wt% SLS as surfactant] for solvent removal at 20°C plotted against total volume fraction of polymer. (——) CSOP; (– – –) CSPO; (· · ·) SHS

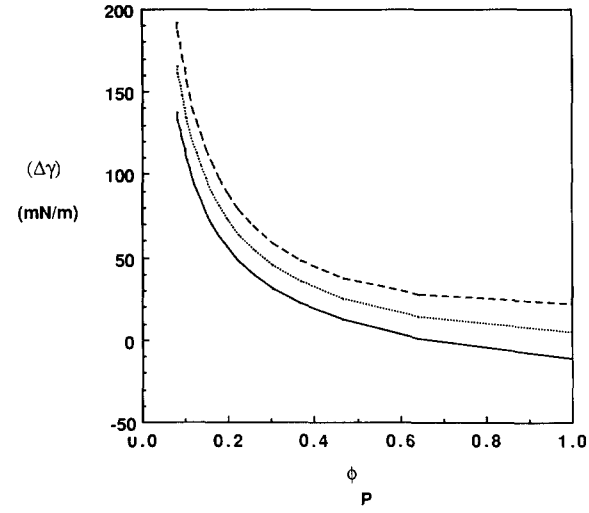

Figure 14 Calculated reduced surface energies [for 50:50 PMMA/PSTY particles swollen with toluene (10 wt% polymer) and suspended in water containing 0.5 wt% MXP as surfactant] for solvent removal at 20°C plotted against total volume fraction of polymer. (——) CSOP; (– – –) CSPO; (· · ·) SHS

2.5 wt% polymer solutions (at higher polymer concentrations, phase separation exists within the solution). SLS (Aldrich) and MXP (Grinsted Products, Denmark) were dissolved at 0.5 wt% in boiled, deionized water. Solvent swollen, single phase, polymer particles of 10–20 μm were formed by emulsifying the polymer solutions into the surfactant solution using a Biospec biohomogenizer. The emulsion was immediately transferred to a stirred reactor, and heated to 40°C to begin removal of the solvent by evaporation. Samples of the emulsion at known degrees of solvent removal were examined for particle morphology using an Olympus BH2 optical microscope equipped with Hoffman modulated objectives.

Results and comparison with theoretical predictions

Photomicrographs of 50:50 PMMA/PSTY particles emulsified with SLS and MXP are shown in *Figures 15* and *16*, respectively, at varying extents of solvent removal. The particles phase separate at low extents of solvent removal. *Figure 15a* (7% solvent removal, $\phi_P = 0.03$) shows that some of the SLS-stabilized particles have phase-separated into distinct hemisphere structures. By 50% solvent removal ($\phi_P = 0.05$, *Figure 15b*) all of the particles are distinct hemispheres; further removal of solvent (78%, $\phi_P = 0.11$, *Figure 15c*) only decreases the particle size (due to the reduction in volume). In contrast, the photomicrographs of *Figure 16*, for MXP-stabilized particles, show the development of a CSOP structure – at no point is there evidence of hemisphere-type morphologies, although some occluded structure may be evident.

In the case of the SLS-stabilized particles, the experimental photomicrographs match the predictions of *Figure 7*, where the hemisphere morphology was

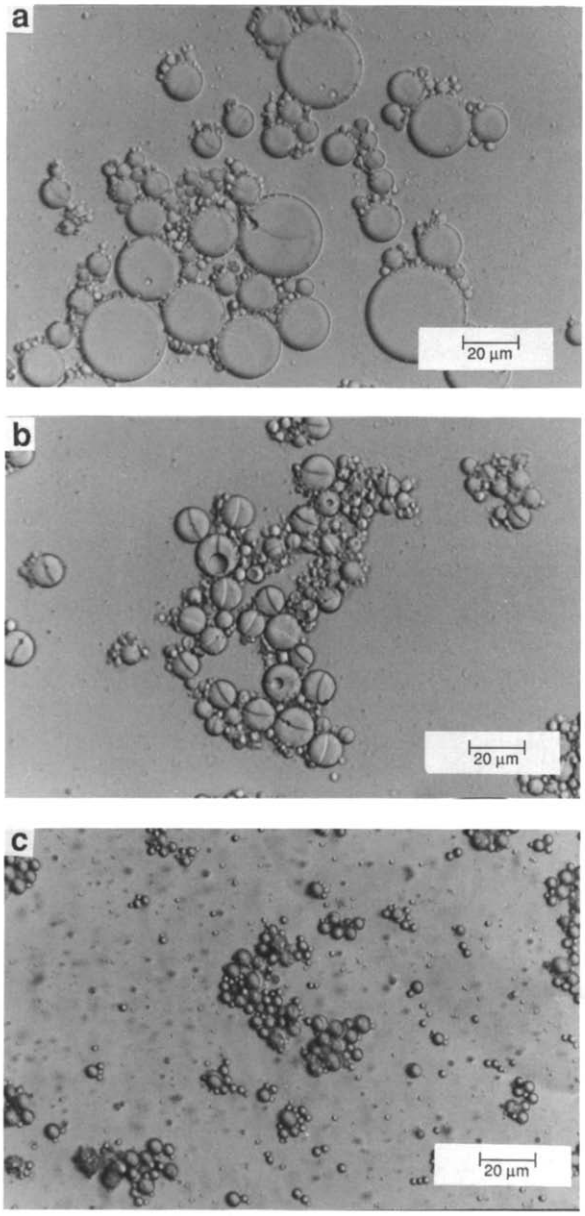

Figure 15 Optical photomicrographs taken during solvent removal at 40°C showing 50:50 PMMA/PSTY particles swollen with $MeCl_2$ and suspended in water containing 0.5 wt% SLS as surfactant. (a) 7% $MeCl_2$ removed; (b) 50% $MeCl_2$ removed; (c) 78% $MeCl_2$ removed

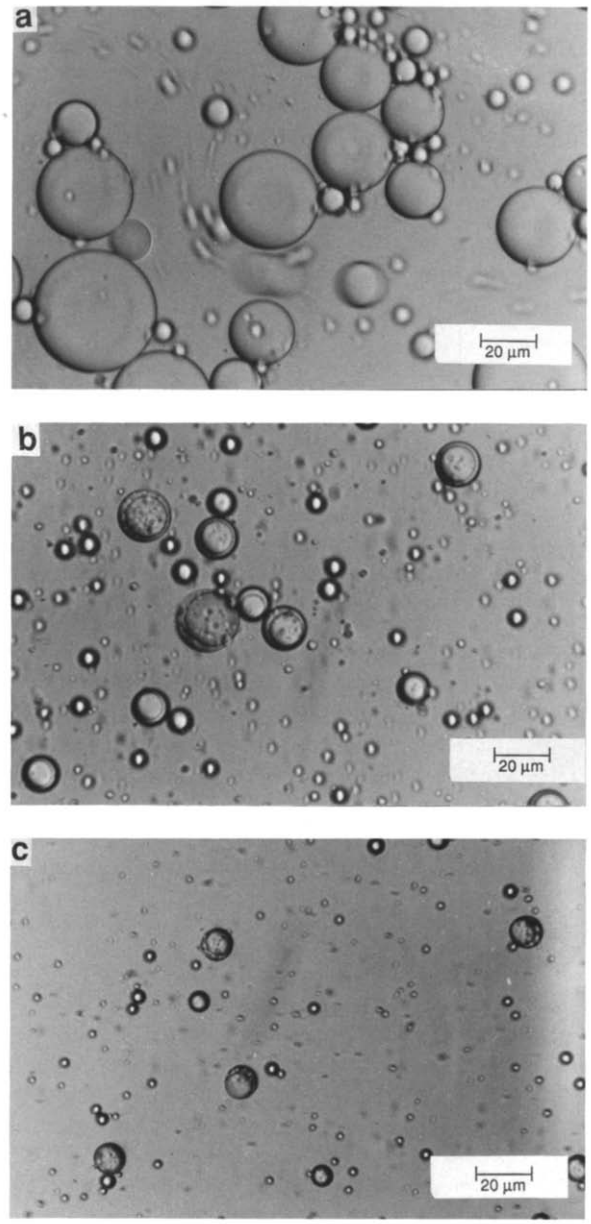

Figure 16 Optical photomicrographs taken during solvent removal at 40°C showing 50:50 PMMA/PSTY particles swollen with $MeCl_2$ and suspended in water containing 0.5 wt% MXP as surfactant. (a) 7% $MeCl_2$ removed; (b) 62% $MeCl_2$ removed; (c) 78% $MeCl_2$ removed

calculated to have the lowest reduced surface energy at all degrees of solvent removal. This was confirmed experimentally (*Figure 15*), despite the closeness of the reduced surface energy curves for the different morphologies. In contrast, *Figure 8*, which shows the calculated reduced surface energies for MXP-stabilized particles, appears to predict HS morphology as the favoured morphology at low polymer volume fractions, with CSOP being favoured at high polymer volume fractions. This is in conflict with the photomicrographs of *Figure 16* which clearly show the formation of CSOP structures throughout the solvent removal process. This latter result indicates the need for exercising caution in determining the 'predicted' morphology when the reduced surface energies are close together, especially when two of the curves appear to cross over one another and suggest a morphology change with extent of solvent removal (or conversion in a reactive system).

Several interesting questions arise when considering morphology development in composite polymer particles formed by artificial processing techniques. The first is the occurrence of occluded morphologies. Although the reduced surface energy curves for occluded morphologies lie close to those of lower reduced surface energy (*Figure 10*), occluded morphologies are rarely observed by us in artificially processed particles when the solvent concentration is high. The large amount of solvent in the particles dramatically decreases the internal viscosity and also the resistance to polymer diffusion would seem to facilitate complete phase separation. In contrast, in reactive-processed particles formed by polymerization of monomer-swollen seed particles, the rapidly increasing viscosity associated with gel and glass effects can possibly lead to 'freezing' of occluded structures even at quite low conversions (i.e. high monomer concentrations). Similarly, it is possible that occlusion formation may occur in artificially processed particles if the rate of solvent removal is very rapid. In both techniques, then, the rate of the process may be important.

A second question that should be considered is the potential influence of the type of solvent on morphology development. Some workers[1,25] have used toluene in seeded emulsion polymerizations to obtain 'thermodynamically stable' morphologies where kinetic control would otherwise lead to occluded, or 'raspberry' particles. The morphology considerations of the preceding section indicate that there can be major effects of the solvent on all of the interfacial tensions and that, depending on the type of solvent and polymers involved, the aqueous interface may be dominated by different species. However, while considering the effects of two solvents with very different polarities, our computations have suggested that one should expect little or no difference between using toluene and $MeCl_2$, even with a variety of surfactants that yield quite different water/polymer phase interfacial tensions. Thus we are led to the tentative conclusion that the type of solvent used will not have an influence upon the particle morphology at any stage of the process. Such a result was not obvious to us at the outset, especially since various solvent/polymer/surfactant combinations can lead to very different interfacial tensions, particularly at the water/particle interface. Much more investigation is required before a firm conclusion can be drawn, and for synthetic latex processing the probable influence of the initiator end groups would have to be considered.

CONCLUSIONS

In this paper we have presented a thermodynamic equilibrium approach for the prediction of equilibrium morphologies of composite particles formed during artificial latex processing. We have demonstrated the importance of considering the effects of solvent on the various interfacial tension and interfacial area components in predicting equilibrium morphologies, although it would appear that equilibrium morphology development may be independent of solvent type.

Experimental observations of particle morphology during quantified solvent removal were made and are in good agreement with the theoretical predictions. However, comparison of the experimentally observed morphologies with the predictions does emphasize a need for exercising some caution in predicting equilibrium morphologies (especially possible morphology changes during processing) where the calculated reduced surface energies are very close together. The presence of large amounts of solvent favours completely phase-separated, basic morphologies (e.g. CSOP, hemisphere) with minimal occlusion formation, in possible contrast to reactively processed systems.

ACKNOWLEDGEMENT

We are grateful for the financial support provided by the donors of the Petroleum Research Fund of the American Chemical Society.

REFERENCES

1 Cho, I. and Lee, K.-W. *J. Appl. Polym. Sci.* 1985, **30**, 1903
2 Lee, D. I. in 'Emulsion Polymers and Emulsion Polymerization' (Eds D. R. Bassett and A. E. Hamielec) American Chemical Society, Washington DC, 1981, p. 405
3 Min, T. I., Klein, A., El-Aasser, M. S. and Vanderhoff, J. W. *J. Polym. Sci., Polym. Chem. Edn* 1983, **21**, 2845
4 Hourston, D. J., Satgurunathan, R. and Varma, H. *J. Appl. Polym. Sci.* 1986, **31**, 1955
5 Hourston, D. J., Satgurunathan, R. and Varma, H. *J. Appl. Polym. Sci.* 1987, **33**, 215
6 Muroi, S., Hashimoto, H. and Hosoi, K. *J. Polym. Sci., Polym. Chem. Edn* 1984, **22**, 1365
7 Lee, D. I. and Ishikawa, T. *J. Polym. Sci., Polym. Chem. Edn.* 1983, **21**, 147
8 Stutman, D. R., Klein, A., El-Aasser, M. S. and Vanderhoff, J. W. *Ind. Eng. Chem. Prod. Res. Dev.* 1985, **24**, 404
9 Okubo, M., Katsuta, Y. and Matsumoto, T. *J. Polym. Sci., Polym. Lett. Edn* 1982, **20**, 45
10 Winzor, C. L. and Sundberg, D. C. *Polymer* 1992, **33**, 3797
11 Sundberg, D. C., Casassa, A. J., Pantazopoulos, J., Muscato, M. R., Kronberg, B. and Berg, J. *J. Appl. Polym. Sci.* 1990, **41**, 1425
12 Hansch, C., Quinlan, J. E. and Lawrence, G. L. *J. Org. Chem.* 1968, **33**, 347
13 Kruse, R. L. in 'Copolymers, Polyblends and Composites' (Ed. N. A. J. Platzer) American Chemical Society, Washington DC, 1975, p. 141
14 Barton, A. F. M. 'CRC Handbook of Solubility Parameters and Other Cohesion Parameters', CRC Press, Boca Raton, 1983, pp. 254–261
15 Broseta, D., Leibler, L., Kaddour, L. O. and Strazielle, C. *J. Chem. Phys.* 1987, **87**, 7248
16 Helfand, E. and Tagani, Y. *J. Polym. Sci.* 1971, **B9**, 741
17 Helfand, E. and Tagani, Y. *J. Chem. Phys.* 1972, **56**, 3592
18 Helfand, E. and Tagani, Y. *J. Chem. Phys.* 1972, **57**, 1812
19 Helfand, E. and Sapse, A. M. *J. Chem. Phys.* 1975, **62**, 1327
20 Russell, T. P., Hjelm, R. P. and Seeger, P. A. *Macromolecules* 1990, **23**, 890
21 Siow, K. S. and Patterson, D. *J. Phys. Chem.* 1973, **77**, 356
22 Prigogine, I. and Marechal, J. *J. Colloid Sci.* 1952, **7**, 122
23 Gaines, G. L. *J. Phys. Chem.* 1969, **73**, 3143

24 Gaines, G. L. *J. Polym. Sci. A2* 1969, **7**, 1379
25 Lee, S. and Rudin, A. *Makromol. Chem., Rapid Commun.* 1989, **10**, 655
26 Kurata, M. and Stockmayer, W. H. *Fortschr. Hochpolym. Forsch.* 1963, **3**, 196
27 Kaddour, L. O., Anastagasti, M. S. and Strazielle, C. *Makromol. Chem.* 1987, **188**, 2223
28 Broseta, D., Fredrickson, G. H., Helfand, E. and Leibler, L. *Macromolecules* 1990, **23**, 132

APPENDIX

This appendix describes the series of calculations necessary for the prediction of particle morphology during a solvent removal experiment. As an example, consider 50:50 (wt/wt) PMMA/PSTY particles swollen with $MeCl_2$ (10 wt% polymer) and suspended in water containing SLS as surfactant. *Table A1* shows the assumed particle composition, both initially, and after removal of 90% of the solvent: subsequent calculations assume the latter condition.

Initially, the composition of each phase must be calculated. Methylene chloride is somewhat water-soluble ($\sim$2 wt%) and therefore partitioning into the aqueous phase will be considered first, since this reduces the amount of solvent available to swell the particles. Defining the aqueous partition coefficient, P, as the ratio of the amounts of solvent in each phase, namely:

$$P = [w_{S,P}/(w_{P1} + w_{P2})]/(w_{S,W}/w_W) \quad \text{(A1)}$$

then it can be shown that:

$$w_{S,P} = (1 - X)w_S/[1 + w_W/P(w_{P1} + Xw_{P2})] \quad \text{(A2)}$$

where X is the fraction of solvent removed. Using equation (A3) with $a = 1.339$ and $b = -0.978$ (ref. 12), P is calculated to be 15.8.

$$\log 1/S = a \log P + b \quad \text{(A3)}$$

Calculation of the amounts of solvent in the polymer ($w_{S,P}$) and aqueous ($w_{S,W}$) phases may lead to the result that the amount of $MeCl_2$ available to partition into the aqueous phase would exceed its aqueous solubility. In such cases, $w_{S,W}$ is set equal to that solubility (0.066 parts in 3.0 parts water), while the remaining $MeCl_2$ ($w_{S,P}$) swells the polymer particles. At 90% solvent removal, $w_{S,W} = 0.063$.

Next the amount of solvent in each polymer phase must be determined. Assuming that the two polymers are equally soluble in $MeCl_2$ and thus selecting $\chi_{PMMA/MeCl_2} = \chi_{PSTY/MeCl_2} = 0.4$ (estimated from solubility parameters[14]) Kruse's equation[13] [equation (A4)] can be used to calculate the volume fractions of polymer in each phase:

$$(1 - v_3)/(1 - v_2) = e^{(\chi_{12} - \chi_{13})} \quad \text{(A4)}$$

The assumption of equal interaction parameters leads to horizontal tie-lines in *Figure 3* and equal volume fractions in each phase. Solving equation (A4) numerically gives $v_2 = v_3 = 0.82$ at 90% solvent removal.

Calculation of the solvent-influenced polymer/polymer interfacial tension requires knowledge of the molecular weights of the two polymers and the polymer/polymer interaction parameter. Complete details of the approach we used (after that of Broseta *et al.*[15]) can be found in our previous paper[10] where we considered the influence of monomer on polymer/polymer interfacial tensions. Using equations (A5)–(A11) and the parameters of *Table A2*, the concentration dependences of $u(c)$ and $\xi(c)$ can be calculated.

$$u(c) = u_0(c/c_K)^{0.3} \quad \text{(A5)}$$

$$u_0 = 2/N_b = 2c_K\xi_K^3/M \quad \text{(A6)}$$

$$\xi(c)/R_g = 0.43(c/c^*)^{-3/4} \quad \text{(A7)}$$

$$c^* = 3M/4\pi R_g^3 N_{AV} \quad \text{(A8)}$$

$$c_K = 227M^{-0.615} \quad \text{(A9)}$$

$$R_g = (\langle R^2 \rangle/6)^{0.5} \quad \text{(A10)}$$

$$\gamma_\infty = (kT/\xi^2)(u/6)^{0.5} \quad \text{(A11)}$$

However, the value of u_0 so calculated, gives $\chi = 0.017$

Table A1 Assumed composition of artificial polymer particles, initially and at 90% solvent removal

Component	Initial (parts)	90% solvent removal (parts)
$MeCl_2$[a]	0.834	0.027
$MeCl_2$[b]	0.066	0.063
PMMA	0.05	0.05
PSTY	0.05	0.05
Water	3.0	3.0
SLS	0.015	0.015

[a] In particles
[b] In aqueous phase

Table A2 Parameters used in the calculation of solvent-influenced polymer/polymer interfacial tension for composite particles at 90% solvent removal

	PSTY	PMMA	Composite	Equation
$\bar{M}_n$	100000	100000	100000	
$\langle R^2 \rangle^{1/2}/M^{1/2}$ (cm g$^{-1/2}$)[a]	6.7×10^{-9}	6.4×10^{-9}		
R_g (cm)	8.65×10^{-7}	8.26×10^{-7}	8.46×10^{-7}	(A10)
c_K (g cm^{-3})[b]			0.191	(A9)
c^* (g cm^{-3})			0.0658	(A8)
ξ_K (cm)			1.701×10^{-7}	(A7)
u_0			0.0108	(A6)
c(blend) (g cm^{-3})			1.116	
u(blend)			0.0171	(A5)

[a] Ref. 26
[b] Ref. 27

Table A3 Parameters used in the calculation of the solvent-influenced polymer/water interfacial tensions for composite particles at 90% solvent removal

	PMMA/$MeCl_2$	PSTY/$MeCl_2$
l[a]	0.5	0.5
m[a]	0.25	0.25
T (°C)	40	40
χ	0.40	0.40
a	2.24×10^{-15}	2.24×10^{-15}
r	1315	1490
ϕ_1	0.18	0.18
ϕ_1^s	0.368	0.383
γ_1 (mN m^{-1})	2.0	2.0
γ_2 (mN m^{-1})[b]	13.1	13.7
γ (mN m^{-1})	9.8	10.2

[a]Ref. 21
[b]Ref. 11

(u calculated for the pure blend), which is somewhat lower than that predicted at 40°C from the temperature dependence [equation (A12)] of Russell *et al.*[20]:

$$\chi = 0.028 + 3.9/T \qquad \text{(A12)}$$

In order to obtain $\chi = 0.04$ (consistent with the experimental measurements of Russell) a revised u_0 ($= 0.0236$) was used. At 90% solvent removal, the polymer concentration (strictly polymer density) is 0.91 g cm^{-3}. Thus $u(0.91) = 0.038$ [equation (A5)], $\xi(0.91) = 5.07 \times 10^{-8}$ cm [equation (A7)] and $\gamma_\infty = 1.33$ [equation (A11)]. In order to obtain the correct molecular weight dependence for interfacial tensions of polymers of equal molecular weight, Broseta *et al.*[28] introduced two additional terms:

$$\gamma = \gamma_\infty(1 - \Delta_1 - u\Delta_2) \qquad \text{(A13)}$$

where γ_∞ is the previously calculated interfacial tension, $\Delta_1 = \pi^2/6w$ and $\Delta_2 \simeq 1.67$. The term w is the incompatibility ($w = \chi N$, where N is the degree of polymerization). For the PMMA/PSTY system considered here, the incompatibility $w = 40$, leading to $\gamma(0.91) = 1.2$ mN m^{-1}.

Calculation of the polymer/water interfacial tensions requires the solution of equation (A14) to obtain ϕ_1^s (the volume fraction of solvent at the interface):

$$\phi_1^s - \phi_1[(1 - \phi_1^s)/(1 - \phi_1)]^{1/r} \exp[(\gamma_2 - \gamma_1)a/kT] + \chi(l + m)(1 - 2\phi_1) + \chi l(2\phi_1^s - 1) = 0 \qquad \text{(A14)}$$

This can be done using numerical techniques (we used the secant method). *Table A3* shows the parameters used to solve equations (A15) and (A16) for the PMMA, $MeCl_2$/water and PSTY, $MeCl_2$/water interfaces:

$$[(\gamma - \gamma_1)a]/kT = \ln(\phi_1^s/\phi_1) + [(r - 1)/r](\phi_2^s - \phi_2) + \chi[l(\phi_2^s)^2 - (l + m)\phi_2^2] \qquad \text{(A15)}$$

$$[(\gamma - \gamma_2)a]/kT = \ln(\phi_2^s/\phi_2)^{1/r} + [(r-1)/r](\phi_2^s - \phi_2) + \chi[l(\phi_1^s)^2 - (l + m)\phi_1^2] \qquad \text{(A16)}$$

At 90% solvent removal, the (equal) volume fractions of solvent in the PMMA and PSTY phases are 0.18; the corresponding calculated interfacial tensions are $\gamma_{PMMA,MeCl_2/H_2O} = 9.8$ mN m^{-1} and $\gamma_{PSTY,MeCl_2/H_2O} = 10.2$ mN m^{-1}.

The final step is to calculate the interfacial areas for the different morphologies. Restricting ourselves to the basic morphologies (CSOP, CSPO and SHS) $(R_{P1}/R_0)^2 = 1.15$ [equation (9)], $(R_{P2}/R_0)^2 = 1.05$ [equation (10)] and $(R_P/R_0)^2 = 1.75$ [equation (8)], while $V_{P2}/V_P = 0.47$ giving $h/R_P = 0.96$ [equations (7) and (11)].

Combining all of this information, the reduced surface energy for each morphology can be calculated at 90% solvent removal [via equations (3), (4) and (6)] giving $(\Delta\gamma)_{CSOP} = 4.67$, $(\Delta\gamma)_{CSPO} = 5.21$ and $(\Delta\gamma)_{SHS} = 4.16$. The predicted morphology would be hemispheres, although it should be noted that all of the reduced surface energies are quite close in value.